EAI Endorsed Transactions
on Energy Web
Research Article EAI.EU

Access Mechanism of Power SDN Controller Based on Multi-level Distributed Control

Yuanjie Liu[1*], Zhongmiao Kang[1], Jiajia Fu[1], Fan Zha[2], Jiakang Guo[2], Guangyu Hu[2]

[1] Guangdong Power Grid Power Dispatching Control Center, Guangzhou, China
[2] NARI Information & Communication Technology Co., Ltd., Nanjing, China

Abstract

INTRODUCTION: With the transformation of the power system towards intelligence and informatization, the traditional single-domain centralized architecture has problems such as high load pressure, poor compatibility and insufficient real-time performance.
OBJECTIVES: In order to enhance the compatibility, real-time performance and multi-level collaborative efficiency of power software-defined network controller access.
METHODS: Using Ant Colony Optimization (ACO) and IGA Immune Genetic Algorithm (IGA) as the core optimization frameworks, this research innovatively constructs an intelligent access model for power software-defined network controllers based on multi-level distributed control.
RESULTS: Experiments show that the load balancing degree and access delay of the research model are 0.898 and 33.4ms respectively, the decision consistency and load migration efficiency are 97.4% and 97.8% respectively, the success rate of parallel access of multi-level controllers is 98.0%, and the average error is 1.51%. Moreover, when multiple numbers and types of controllers are connected, the interface matching degree exceeds 80.00%. Meanwhile, the anti-interference ability and compatibility of the research model are both superior to those of the comparison model.
CONCLUSION: The research model provides an efficient solution for the intelligent access of power software-defined network controllers and contributes to promoting the high-quality development of power communication networks.

Keywords: Regional-level collaborative access, PPO-FC-ACO, Resource scheduling, TS-IGA, Access path optimization

Received on 14 May 2026, accepted on 15 July 2026, published on 07 September 2026

doi: 10.4108/ew.13020

*Corresponding author. Email: lyj1234202512@163.com

1. Introduction

As the power system continues to move toward intelligence and informatization, the power communication network, which plays a key role in ensuring the safe operation of the system, faces many challenges. Software Defined Network (SDN), with its programmable and centralized management capabilities, has gradually become a core technology in the power industry [1–2]. However, due to the large scale of power networks and the high demands for real-time performance and security, the traditional single-domain centralized SDN controller architecture encounters limitations in control coverage and faces significant load pressure during access, highlighting the need for a controller access method that supports both global coordination and local adaptation [3]. Ant Colony Optimization (ACO), inspired by the way ant colonies cooperate by secreting and sensing pheromones while foraging, is effective in solving complex combinatorial optimization problems and is widely used in industrial scheduling and communication networks [4]. Immune Genetic Algorithm (IGA) builds on traditional genetic algorithms by incorporating mechanisms such as antigen recognition and immune memory, which help maintain diversity and efficiency among antibodies and overcome issues like local optima and slow convergence [5]. Based on ACO and IGA, this paper introduces Fuzzy Control (FC), Proximal Policy Optimization (PPO), and Tabu Search (TS) to improve both algorithms, forming two hybrid algorithms. These are further integrated into a fused algorithm, which is then used to construct an intelligent access model for power SDN controllers based on multi-level distributed control. The aim is to address the problems existing in the traditional controller access methods, such as weak compatibility of multiple types of heterogeneous controllers and high access delay in dynamic scenarios. The innovation of this research lies in the following three points: Firstly, it designs a hierarchical collaborative optimization strategy for the differentiated design of the power SDN global layer - regional layer - device layer architecture, achieving the linkage and collaboration of upper and lower-level controllers for access. Secondly, it combines PPO, FC and ACO to form PPO-FC-ACO, which is used to solve the real-time decision-making problems in the dynamic uncertain scenarios of the regional layer, and combines TS and IGA to form TS-IGA, achieving the joint optimal scheduling of access resources and transmission paths. Thirdly, the multi-algorithm composite framework is successfully applied to the power-specific SDN network, taking into account the actual needs of high real-time performance, high reliability and heterogeneous access of multiple devices for power business.

2. Related works

As a heuristic global optimization algorithm inspired by the foraging behavior of ants, ACO was able to perform global optimization on controller access paths in the regional control layer. Based on this, many scholars at home and abroad carried out related research. For example, to solve the problem of how to place SDN controllers to improve network performance in power systems, Frdiesa et al. put forward a controller placement method based on ACO. The study found that this method showed better performance in terms of both global delay and delay between controllers [6]. To address the issue of unreasonable path planning for spot welding robots using ACO, Tan et al. combined ACO with the Particle Swarm Optimization algorithm and trained the parameters of ACO to obtain the optimal path. Experiments showed that the improved ACO algorithm achieved higher solution quality and faster convergence speed [7]. IGA is a hybrid heuristic optimization algorithm that combines principles of the biological immune system with the structure of genetic algorithms. It effectively improves the performance in solving complex combinatorial optimization problems. For instance, Sharifi et al. developed a multi-state component series-parallel system based on immune algorithms to address the redundancy reliability allocation problem. The results showed that this system effectively reduced the cost of redundant reliability allocation [8]. To design a secure substitution box (s-box) with high nonlinearity and low differential uniformity, Behera et al. proposed a hybrid algorithm based on genetic algorithms. The study found that the s-box generated by this algorithm had better nonlinearity and significantly improved the security of block ciphers [9]. Overall, the existing studies have mainly focused on improving the ACO algorithm in a single-path optimization scenario, without integrating techniques such as reinforcement learning and fuzzy control that are suitable for the dynamic and variable operating conditions of power networks, making it difficult to support the collaborative decision-making of multi-level controllers.

At present, research on power SDN controllers has made some progress, and many scholars have not only explored optimization methods but also applied them in practical scenarios. For example, to efficiently and flexibly monitor the network traffic of SDN controllers, Ram et al. proposed a structural design method based on the RYU SDN controller. The study showed that this method enabled clear observation of controller-related data such as round-trip time, bandwidth, and throughput [10]. To solve the network delay and reliability issues in the controller placement process, Singh et al. put forward a network model based on the Particle Swarm Optimization algorithm. Results showed that this model significantly improved the placement efficiency of SDN controllers [11]. To address the potential security risks brought by Dynamic Host Configuration Protocol (DHCP) to SDN controllers, Ishtiaq et al. proposed a DHCP security algorithm based on the RYU controller to reduce the impact of DHCP attacks. Results showed that this method improved CPU utilization by 93.9% and reduced the packet loss rate by 95% [12]. In conclusion, although certain achievements have been made in the research on SDN controllers at present, there are still some limitations: The research on power SDN controllers mainly focuses on aspects such as single-point deployment of the controller, traffic monitoring, and single security protection. The mainstream models and algorithms are all designed for single-domain centralized architectures, ignoring the hierarchical collaborative requirements of the multi-level distributed network architecture of the power system.

Therefore, by introducing PPO, FC and TS respectively to improve ACO and IGA, two hybrid algorithms were obtained, and they were combined to form a fusion algorithm. At the same time, an intelligent access model for power SDN controller based on multi-level distributed control was constructed. Compared with the existing research designs that simply superimpose multiple algorithms or operate independently in modules, the two types of hybrid algorithms designed in this study achieved a deep integration of algorithm mechanisms and iterative logic: the core operation rules of PPO, FC and TS were embedded into the full-process iterative optimization of ACO and IGA, forming a new architecture with bidirectional closed-loop linkage.

3. Intelligent access model for power SDN controllers

3.1 PPO-FC-ACO design for regional-level optimization and collaborative access

Power SDN typically adopts a multi-level distributed architecture composed of a global layer, a regional layer, and a device layer. As the middle layer, the regional layer plays a core role in coordinating network resources and processing real-time services [13]. However, it also faces strong uncertainty in network state and lacks dynamic adaptability, which requires further optimization. ACO, with its group-based optimization and dynamic path planning capabilities, is well-suited for optimizing access paths of controllers in the regional layer. FC simulates fuzzy thinking in human decision-making and helps controllers handle the complexity and high uncertainty in the regional layer. This study combines ACO with FC to form the FC-ACO hybrid algorithm, which reduces the uncertainty and enhances the adaptability of the regional layer. The structure of FC-ACO is shown in Figure 1.

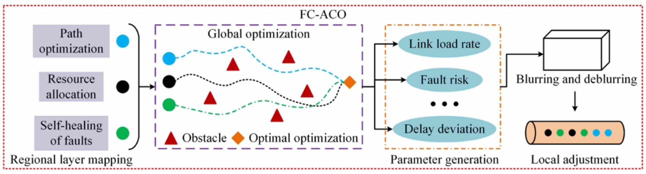

Figure 1. Structure of the FC-ACO hybrid algorithm

As shown in Fig. 1, FC-ACO first uses ACO to simulate ants foraging behavior and maps the parameters of the regional layer into ant individuals. It abstracts the optimization problem into obstacles and finds optimal parameters through ACO. Then, FC performs fuzzification and defuzzification on parameters such as link load rate and fault risk, enabling dynamic adjustment of local parameters. This process improves the real-time performance and reliability of the regional layer. The ACO process of selecting the shortest path is expressed in Equation (1).

$$P_{ij}^{k}(t)=\begin{cases}\dfrac{|\tau_{ij}(t)|^{\alpha}\cdot|\eta_{ij}(t)|^{\beta}}{\sum_{s\in k}|\tau_{is}(t)|^{\alpha}\cdot|\eta_{is}(t)|^{\beta}} & \text{if } j\in k\\ 0 & \text{otherwise}\end{cases} \quad (1)$$

In Equation (1), $P(\cdot)$ is defined as the probability of the ant's path selection, with a value range of [0, 1], $\tau_{ij}(t)$ represents the pheromone concentration from node i to j at time t. $\eta(\cdot)$ is the heuristic function, and α and β are the weight coefficients of the pheromone and the heuristic function respectively. The value range for both is (0, 5]. k denotes the set of unvisited nodes. The dynamic adjustment of parameters optimized by ACO using FC is shown in Equation (2) [14].

$$\begin{cases}a(t)=a_0-\Delta a_{FC}\\ b(t)=b_0+\Delta b_{FC}\\ c(t)=c_0+\Delta c_{FC}\end{cases} \quad (2)$$

In Equation (2), a, b, and c are optimized parameters. Δa_{FC}, Δa_{FC}, Δb_{FC}, and Δc_{FC} are all parameters to be optimized. a_0, b_0, and c_0 are the adjustment amounts of FC, and their value range is [-0.2, 0.2]. After optimizing the regional layer, the study combines FC-ACO with PPO to enhance the capability of multi-level distributed controller access, forming PPO-FC-ACO. The specific process is shown in Fig. 2.

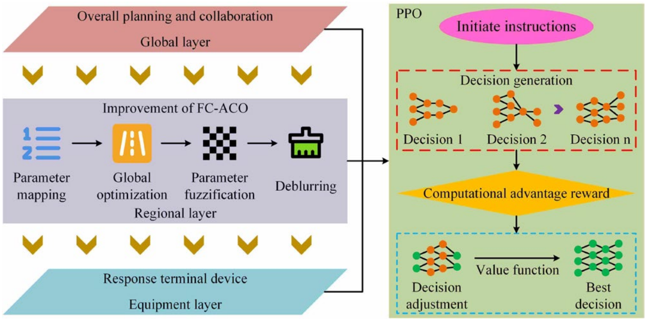

Figure 2. Collaborative access process for multi-level SDN controllers based on PPO-FC-ACO (Icon source from: https://iconpark.oceanengine.com/home)

As shown in Fig. 2, during controller access under multi-level distributed control, PPO first determines access priority and generates access decisions based on the status of each layer. It then updates the decision using clipping techniques and advantage functions. When the instruction from the global layer is sent to the regional layer, FC-ACO adjusts parameters in the instruction and FC generates the optimal access decision for the regional controller, which is then executed in the device layer to complete the controller access process. The reward function used by PPO during optimization is shown in Equation (3) [15].

$$r=\omega_1\cdot r_{load}+\omega_2\cdot r_{delay}+\omega_3\cdot r_{\mathrm{reliability}} \quad (3)$$

In Equation (3), r is the reward function. r_{load} is the load balancing reward. r_{delay} is the delay optimization reward. $r_{\mathrm{reliability}}$ is the performance reliability reward. ω is the weight coefficient. The range of values is (0, 1). The update process using clipping techniques is shown in Equation (4) [16].

$$A(S_t,v_t)=Q(S_t,v_t)-V(S_t) \quad (4)$$

In Equation (4), $A(S_t,v_t)$ is the policy update function. $V(S_t)$ is the state value function. $Q(S_t,v_t)$ is the probability of taking action v under state S. The process of generating the optimal access decision using clipping is described in Equation (5) [17].

$$L_{CLIP}(\theta) = \mathrm{IE}\left[\begin{array}{l}\min(\frac{\pi_\theta(v_t|S_t)}{\pi\theta_{old}} \cdot A(S_t, v_t), \\ \mathrm{clip}(\frac{\pi_\theta}{\pi\theta_{old}}, 1-\varepsilon, 1+\varepsilon) \cdot A(S_t, v_t)\end{array}\right] \quad (5)$$

In Equation (5), $L_{CLIP}(\theta)$ is the objective function. θ_{old} is the old policy parameter. ε is the clipping coefficient within [0,1], used to limit the update range.

3.2 The intelligent access model for SDN controllers based on multi-level distributed control

Although PPO-FC-ACO improves regional layer coordination and supports multi-level controller access, it cannot effectively schedule resources or optimize access paths. To solve this problem, the study introduces IGA. IGA simulates the immune system's process of recognizing and eliminating antigens using antibody coding to retain high-quality solutions and suppress similar or poor solutions, thus improving solution quality. However, IGA alone tends to fall into local optima and needs enhancement. TS, by simulating human memory and forgetting mechanisms, helps prevent the algorithm from becoming trapped in local optima and improves computational security [18]. Therefore, the study combines TS with IGA to form the TS-IGA hybrid algorithm. Its structure is shown in Fig. 3.

Figure 3. Structure of the TS-IGA hybrid algorithm

As shown in Fig. 3, TS-IGA begins by encoding resources and access paths into antibodies through IGA to initialize the population and calculate affinity. Then, antibodies with high affinity are selected to generate the next generation via reproduction and mutation, enhancing diversity and eliminating poor solutions. TS generates neighborhood solutions based on the output of IGA and uses a tabu list to reduce complexity. Finally, it applies an aspiration criterion to re-explore tabu solutions to avoid missing optimal results and obtains the best access strategy. The process of calculating antibody affinity is shown in Equation (6).

$$\mathrm{Affinity}(x) = \frac{1}{1+F(x)} \quad (6)$$

In Equation (6), $\mathrm{Affinity}(x)$ represents antibody affinity. $F(x)$ is the antigen. IGA selects high-quality antibodies based on their affinity and concentration in Equation (7).

$$Concentration(x_{i'}) = \frac{1}{N}\sum_{N=1}^{N} sim(x_{i'}, x_{j'}) \quad (7)$$

In Equation (7), $Concentration(x_{i'})$ denotes the selection process for antibody $x_{i'}$. N is the size of the antibody population. The range of values is from 20 to 200. $sim(x_{i'}, x_{j'})$ is the similarity between antibodies $x_{i'}$ and $x_{j'}$. The process of TS generating neighborhood solutions using IGA is shown in Equation (8) [19].

$$y_{\mathrm{neighbor}} = y_{\mathrm{current}} + \Delta y \quad (8)$$

In Equation (8), y_{neighbor} is the neighborhood solution. y_{current} is the current optimal solution from IGA. Δy is a random disturbance value. The range of values is from -0.1 to 0.1. Since PPO-FC-ACO focuses on optimizing the regional layer and coordinating multi-level distributed access, while TS-IGA addresses resource scheduling and path optimization, neither alone provides a complete access solution. Therefore, the study integrates the two into a fused algorithm to achieve efficient SDN controller access. The process is illustrated in Fig. 4.

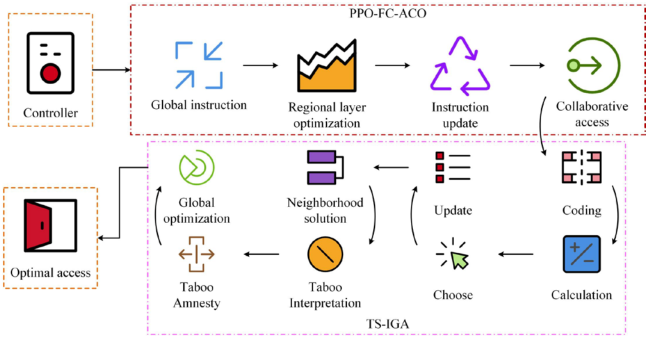

Figure 4. Access process of SDN controllers using the fused algorithm (Icon source from: https://iconpark.oceanengine.com/home)

In Fig. 4, PPO first generates a global access instruction and updates decisions in real time according to the state of each controller layer, supporting multi-level distributed access. Then, TS-IGA dynamically optimizes resource scheduling and path assignment through encoding and affinity evaluation. Finally, the tabu list and aspiration criteria in TS improve the global optimal probability of the access decision, avoiding local optima. The fused algorithm considers multiple targets, such as resource utilization and time delay. The target function is shown in Equation (9).

$$\min F'(x') = w_1 \cdot C(x') + w_2 \cdot D(x_2) \qquad (9)$$

In Equation (9), $\min F'(x')$ is the objective function of the decision variable x'. $C(x')$ is the cost of resource scheduling. $D(x')$ is the transmission delay. w_1 and w_2 are weight coefficients. The range of values is (0, 1). The structure of the TS tabu list is expressed in Equation (10) [20].

$$\text{Tabu} = \{X_1, X_2, \cdots, X_T\} \qquad (10)$$

In Equation (10), Tabu is the tabu list. X is the searched solution. T is the tabu length. Based on the fused algorithm of PPO-FC-ACO and TS-IGA, the proposed model balances global optimization and local adjustment and effectively solves core problems during controller access. The access process is shown in Fig. 5.

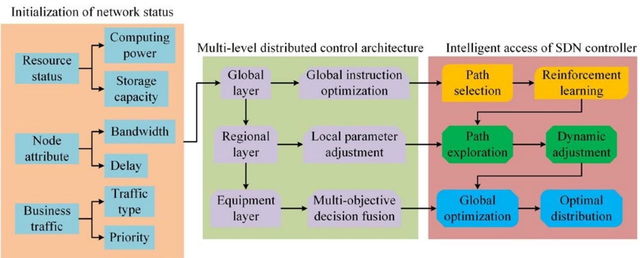

Figure 5. Intelligent access process of SDN controllers using the proposed model

As can be seen from Figure 5, the first step is to establish a multi-level distributed control architecture consisting of the global layer, regional layer, and device layer. The output of the PPO-FC-ACO module is used as the initial input for the TS-IGA module. Subsequently, the PPO module completes the iterative update of the global decision instructions, while the FC-ACO module optimizes the access path and performs preliminary resource allocation based on the input parameters, and the FC module combines with ACO to complete the preliminary conflict resolution. Then, the TS-IGA module receives the path schemes and resource allocation results from the upstream output, and through operations such as antibody affinity screening and constraint of the forbidden table, it avoids local optimality of the algorithm and corrects access conflicts. Finally, the unified controller access decision is generated by integrating the multi-level optimization results, conflict handling results, and multi-objective evaluation indicators, and is then issued to all levels of the entire network to complete the intelligent access of the power SDN controller. IGA introduces the concept of immune mutation to enhance solution diversity. This is expressed in Equation (11).

$$R_{mut}(x_{i'}) = \gamma \cdot \text{Concentration}(x_{i'}) + \delta \qquad (11)$$

In Equation (11), $R_{mut}(x_{i'})$ defines the mutation of antibody $x_{i'}$. γ and δ are adjustment coefficients. TS determines whether to accept the neighborhood solution using an acceptance rule shown in Equation (12).

$$x^*_{new} = \begin{cases} x^*_{\text{neighbor}} & \text{if } F'(x^*_{\text{neighbor}}) < F'(x^*_{\text{current}}) \\ x^*_{\text{current}} & \text{otherwise} \end{cases} \qquad (12)$$

In Equation (12), x^*_{new} is the acceptance rule. x^*_{neighbor} is the neighborhood solution of TS. x^*_{current} is the current best solution. $F'(\cdot)$ is the objective function.

The research model is designed as a framework combining a three-layer distributed physical architecture with a two-layer algorithmic logical architecture. The physical layer is divided into three levels: the global layer, the regional layer, and the device layer, representing the overall power SDN network architecture. The global layer deploys the master control unit to issue overall access instructions and perform global status monitoring. Each regional layer deploys an independent regional controller to receive instructions and complete local network parameter optimization. The device layer connects various heterogeneous power terminals and sub-controllers. The algorithmic logical architecture is divided into a collaborative decision-making layer and a resource scheduling layer. The collaborative decision-making layer uses the PPO-FC-ACO algorithm to achieve multi-level interaction, dynamic decision-making, and preliminary path optimization. The resource scheduling layer uses the TS-IGA algorithm to complete access resource allocation, deep optimization of transmission paths, and avoidance of local optimal solutions.

4. Performance verification and application evaluation

4.1 Algorithm Parameter Settings and Selection Basis

The main parameter settings for the PPO-FC-ACO algorithm are as follows: The ACO module sets the pheromone weight coefficient to 1.2, the heuristic function weight coefficient to 2.0, the pheromone evaporation coefficient to 0.15, and the number of ant populations to 45. The parameter adjustment range for the FC module is limited to the interval [-0.2, 0.2], and a triangular membership function with a step size of 0.02 is used to complete the fuzzy and defuzzification processing. The PPO module sets the load balancing, delay optimization, and reliability reward weights to 0.4, 0.35, and 0.25 respectively, and the clipping coefficient to 0.2. The training rounds are set to 800, and the step size and batch size of the advantage function are 16 and 32 respectively. At the same time, the command issuance cycle from the global layer to the regional layer is set to 10ms, the parameter adjustment cycle of the regional layer is 5ms, and the output interval of the single access decision is 20ms. The above parameters are set based on the operational characteristics and actual requirements of the power SDN network, taking into account the algorithm's optimization ability, operational stability, and real-time performance of the business.

The main parameter settings of the TS-IGA algorithm are as follows: The IGA module sets the antibody population size to 80, the antibody similarity threshold to 0.7, the two adjustment coefficients of immune variation to 0.12 and 0.08 respectively, the crossover probability to 0.7, and the mutation probability to 0.06. The TS module sets the infeasibility length to 12, the random disturbance range of neighborhood solutions to [-0.1, 0.1], the single-step disturbance increment to 0.01, and generates 20 neighborhood solutions in each iteration, and adopts the optimal solution amnesty criterion. In addition, the TS-IGA algorithm combines the resource scheduling cost weight in the objective function to 0.55 and the path transmission delay weight to 0.45. These parameter settings have taken into account the actual requirements for power SDN resource scheduling and path optimization, and are conducive to balancing the solution accuracy, population diversity, and search efficiency.

4.2 Performance evaluation of the PPO-FC-ACO hybrid algorithm

To evaluate the performance of PPO-FC-ACO, the study compared it with Improved Particle Swarm Optimization (IPSO), Deep Deterministic Policy Gradient (DDPG), and Genetic Algorithm combined with Multi-Agent Reinforcement Learning (GA-MARL). To ensure the fairness of the comparative experiments and the reliability of the experimental results, all the comparison algorithms are deployed in the same software and hardware environment as PPO-FC-ACO, and the same test data set, network topology, simulation conditions and iteration termination criteria are adopted. At the same time, a unified parameter grid optimization is conducted for the three comparison algorithms, and the most optimal parameter configuration is determined by traversing the mainstream parameter combinations to minimize the experimental deviation.

The hardware environment of the simulation test platform is Windows 11 Professional operating system, Intel Core i5-14600KF CPU, NVIDIA RTX 5060Ti 8GB GPU, 64GB DDR4 3600MHz memory and 2TB solid-state drive storage. The software development environment uses Python 3.8, combined with mainstream SDN simulation components and power network simulation tools to complete algorithm deployment, data collection and index calculation. The background redundant programs are all turned off throughout to ensure the stability and interference-free of the experimental environment. The experimental data set is the IEEE RTS-96 standard power test data set. This data set is a common classic example in the field of power systems, including 9 core nodes, 32 transmission lines, 17 power generation units, load nodes and other complete topologies and equipment parameters. It can simulate normal grid operation, line faults, load sudden changes and other more than ten typical working conditions, and can fully reproduce the collaborative access process of multi-level SDN controllers in different grid loads and fault scenarios.

The algorithm deployment process is as follows: Firstly, set up the underlying simulation environment. Configure the Python 3.8 runtime environment, SDN simulation component, and power network simulation tool in the Windows 11 system, and complete the import of the IEEE RTS-96 dataset and the initialization of the network topology. Secondly, deploy the algorithm modules, load the PPO decision module, the FC fuzzy control module, and the ACO ant colony optimization module in sequence, and complete the interface coordination and parameter initialization of the three modules. Then, set the main parameters of the algorithm model, focus on the hardware resources, and close the redundant background programs. Finally, start the simulation experiment, and complete the data collection and calculation of indicators such as regional layer load, delay, and decision consistency in the order of iterations. The study first compared the four algorithms in terms of load balancing and access delay in the regional layer. The results are shown in Fig. 6.

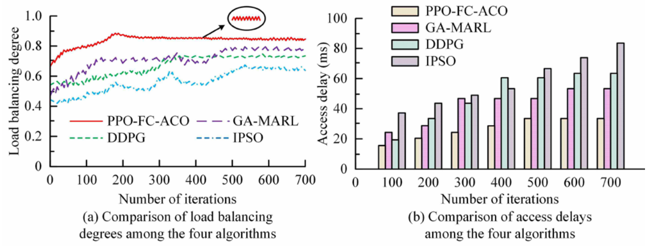

Figure 6. Comparison of regional-layer load balancing and access delay

As shown in Fig. 6(a), PPO-FC-ACO achieved a maximum load balancing value of 0.898 at the 178th iteration, with an average value of 0.862, significantly outperforming the other algorithms. This was because the hybrid algorithm effectively combined the dynamic decision-making ability of PPO, the uncertainty-handling ability of FC, and the global optimization ability of ACO, making it more suitable for the load characteristics of the regional layer and multi-level controller coordination. From Fig. 6(b), it was observed that the access delay of PPO-FC-ACO reached a maximum of 33.4ms at the 500th iteration and remained stable afterwards. This was mainly due to the hybrid algorithm's capacity to integrate the strengths of all three algorithms, enabling real-time access path optimization and suppressing the effects of uncertainty. Next, the study conducted comparative experiments on decision consistency and load migration efficiency during multi-level controller access. The results are shown in Fig. 7.

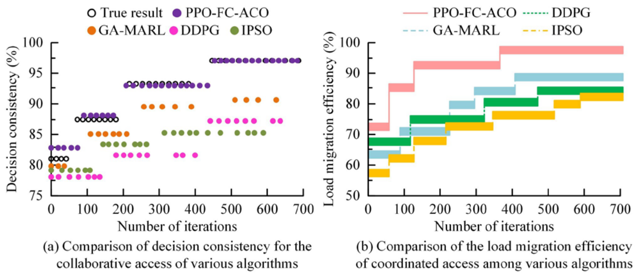

Figure 7. Comparison of decision consistency and load migration efficiency

As shown in Fig. 7(a), PPO-FC-ACO achieved decision consistency closer to the actual access results, with a maximum value of 97.4%. Fig. 7(b) showed that its load migration efficiency peaked at 97.8% at the 360th iteration. These results outperformed the other algorithms, primarily because PPO-FC-ACO integrated the decision-making ability of PPO, the uncertainty-handling ability of FC, and the global optimization capacity of ACO. This combination ensured consistent decision logic and efficient load migration paths during controller coordination. Overall, PPO-FC-ACO demonstrated stronger real-time decision-making and resource allocation capabilities. It balanced global search for regional optimization with local adjustments during multi-level distributed controller access, contributing to the efficient and stable operation of power SDN controllers.

4.3 Effectiveness evaluation of the intelligent SDN controller access model

After verifying the performance of PPO-FC-ACO, the study further validated the proposed model by comparing it with Graph Convolutional Network and Long Short-Term Memory (GCN-LSTM), Counterfactual Multi-Agent Policy Gradients (COMA), and Deep Q-Network and Genetic Algorithm (DQN-GA). The actual measurement experiment strictly adhered to the principle of equal comparison: The four types of models were deployed in the same physical network, the same controller cluster, and heterogeneous terminal devices. The parameters such as network bandwidth, topology structure, number of access devices, interference type and intensity were all completely unified. At the same time, all the comparison models were optimized with the same specifications of parameters, and the access permissions, protocol adaptation rules and data collection standards were unified to ensure consistent experimental conditions.

The field test adopted H3C wide-area SDN as the real test platform. The test environment was divided into three layers: the power communication core area, edge access area and terminal device area. A total of 1 global master controller, 6 regional sub-controllers and more than 40 heterogeneous power terminal devices were deployed, covering mainstream commercial power SDN controllers, traditional industrial controllers and other heterogeneous devices. The network bandwidth was fixed at 1000 Mbps, and the network topology adopted a typical tree-mesh hybrid architecture widely used in the power industry, which conforms to the actual networking form of prefecture-level power wide area networks. Model deployment follows a hierarchical and step-by-step launch rule: First, the on-site network setup is completed, constructing a three-layer physical network consisting of the power communication core area, edge access area, and terminal equipment area. Then, the global master controller, regional sub-controllers, and heterogeneous terminal devices are deployed, with a 1000Mbps fixed bandwidth and a tree-mesh hybrid topology configured. Next, the overall deployment of the fusion algorithm is carried out, uploading the PPO-FC-ACO and TS-IGA modules for data interaction, completing the device protocol and interface adaptation, and simultaneously configuring interface and protocol matching for multiple types of heterogeneous controllers, and completing access permissions and security policy settings. Finally, load testing and actual measurement experiments are conducted, and real measurement data is collected simultaneously. The study first conducted a comparative experiment on the success rate and error of the parallel access of four models' multi-level controllers, and the results are shown in Figure 8.

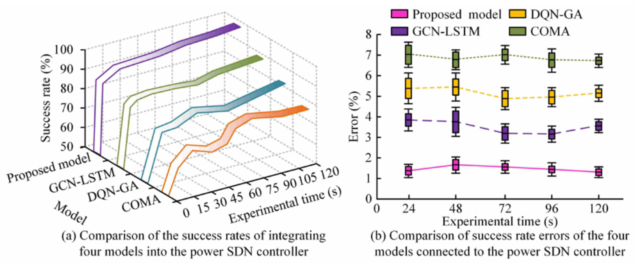

Figure 8. Comparison of access success rate and error for SDN controller access

In Fig. 8(a), the proposed model achieved the highest multi-level controller access success rate of 98.0%, significantly outperforming GCN-LSTM (89.5%), DQN-GA (83.6%), and COMA (78.8%). Fig. 8(b) showed that the access error of the proposed model remained lower than the other models throughout the test, peaking at 1.67% at 48 seconds, with an average error of 1.51%. These results were mainly due to the proposed model's ability to use TS-IGA for global optimization and local fine-tuning, which effectively reduced access conflicts and deviations caused by imbalanced resource allocation. The study then compared the interference resistance of each model during multi-level controller access. The results are shown in Table 1.

Table 1. Response time comparison of access decisions under different interference types

Interference type	Status	Response time (ms)			
		Research model	GCN-LSTM	COMA	DQN-GA
Environmental	Before interference	125.8	182.9	201.3	210.8
	After interference	143.6	237.2	316.1	285.4
Dos attack	Before interference	125.8	182.9	201.3	210.8
	After interference	182.0	294.8	467.9	438.2
Data tampering	Before interference	125.8	182.9	201.3	210.8
	After interference	194.7	321.3	435.6	443.9

In Table 1, the response time of the proposed model before interference was 125.8ms. Under environmental interference, Dos attacks, and data tampering, the response times were 143.6ms, 182.0ms, and 194.7ms, respectively. The largest increase occurred under data tampering (51.1ms), while the smallest was under environmental interference (17.8ms). These results demonstrated the model's strong resistance to environmental interference and its ability to defend against network attacks to some extent. This is because when a DoS attack triggers a large number of redundant packets and link congestion is detected, PPO-FC-ACO can dynamically adjust access permissions and transmission paths, divert malicious traffic, and thereby prevent controller resources from being maliciously occupied. At the same time, the TS-IGA algorithm, during the process of resource scheduling and path optimization, will perform multi-dimensional feature verification on the interaction data and control instructions, and through the antibody recognition mechanism of IGA, filter out tampered data, and defend against data tampering attacks from both the dimensions of data verification and path isolation. Finally, the study compared the interface compatibility of each model during multi-level controller access. The results are shown in Fig. 9.

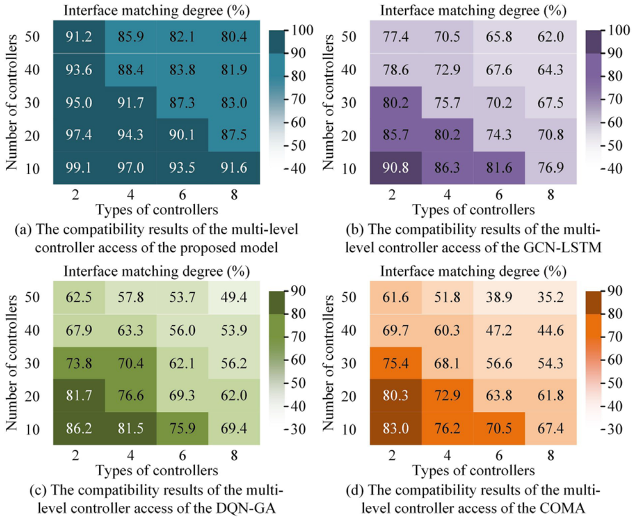

Figure 9. Comparison of interface matching degree in multi-level controller access

As shown in Fig. 9(a), the minimum interface matching degree of the proposed model was 80.4%. When accessing two types of controllers, the matching degree exceeded 90%, indicating a high degree of consistency in protocol specifications and data formats, allowing for plug-and-play functionality without additional modifications. Figures 9(b) to 9(d) showed that when the number of controller types increased to 8 and the number of controllers reached 50, COMA had the lowest interface matching degree at only 35.2%. This indicated that COMA required substantial adaptation to ensure compatibility; otherwise, communication failures or data loss might occur. In summary, the proposed model enabled more accurate controller coordination and stronger resistance to interference during multi-level distributed SDN controller access. It also demonstrated high reliability, strong compatibility, and excellent stability, contributing to improved efficiency and stability of power network operations.

4.4 Ablation Experiments and Parameter Sensitivity Analysis

To quantitatively verify the contributions of the three modules (PPO, FC, TS) and their respective sub-modules to the overall access performance of the model, multiple ablation control groups were set up. Using the fully integrated model as the benchmark, individual/combined modules were sequentially removed, and comparative tests were conducted under unified experimental conditions. The evaluation indicators selected were load balancing degree, access delay, decision consistency, and access success rate. The results are shown in Table 2.

Table 2. The results of the ablation experiment

Interference type	Experimental indicators			
	Load balancing degree	Access delay/ms	Decision Consistency/%	Access success rate/%
Full Model	0.898	33.4	97.4	98.0
No PPO	0.752	51.7	84.1	85.3
No FC	0.813	42.2	89.5	90.6
No TS	0.786	46.9	86.7	87.2
No PPO+FC	0.645	68.3	72.3	74.1
No TS+FC	0.701	62.5	78.2	79.5

As shown in Table 2, after removing the PPO module, the access delay increased by 18.3 ms, the decision consistency and access success rate decreased by 13.3% and 12.7% respectively, and the load balance degree dropped to 0.752, indicating that PPO is the core module for multi-level controller collaborative decision-making and dynamic priority scheduling. When the FC module was removed, the four indicators were also worse than the complete model, confirming that FC is an important unit for improving the adaptability of heterogeneous controllers and optimizing local load balance. After removing the TS module, the model was prone to fall into a local optimal solution, and the load balance degree and decision consistency significantly decreased, indicating that the taboo search and amnesty criteria of TS can effectively compensate for the defect of IGA being prone to local convergence. However, when both the TS module and the FC module were removed simultaneously, the model performance dropped sharply, with the access delay exceeding 60 ms and the access success rate being less than 75%. These results fully demonstrate that the absence of any module will disrupt the overall operational logic of the model, verifying the rationality and necessity of the multi-algorithm integration architecture design.

Furthermore, the study conducted a time complexity analysis on the two hybrid algorithms, PPO-FC-ACO and TS-IGA, and compared the computational costs of the overall fusion model. The size of the ant/antibody population was defined as N, the maximum number of iterations of the algorithm as G, the dimension of the problem solution as D, and the number of neighborhood solutions generated by the TS algorithm in a single iteration as M. The computational complexity analysis of the PPO-FC-ACO algorithm is as follows: In each iteration of ACO, a single ant traverses all D nodes to complete the path search. The time complexity per generation is $O(N \cdot D)$, and after G iterations, the complexity is $O(G \cdot N \cdot D)$. The FC module only performs fuzzification and defuzzification operations on the output parameters of ACO, and the computational load is linearly related to the solution dimension, with a complexity of $O(D)$, which is a low-cost operation. The time complexity for PPO strategy update, advantage function calculation, and sample sampling is $O(G \cdot N)$. In summary, since $O(G \cdot N \cdot D)$ is the highest order term, the overall time complexity of PPO-FC-ACO is $O(G \cdot N \cdot D)$.

The computational complexity of the TS-IGA algorithm is as follows: In the IGA module, the time complexity for population initialization, fitness calculation, and crossover/mutation operations is $O(G \cdot N \cdot D)$, while in TS, generating M neighborhood solutions based on the optimal solution of IGA, maintaining the taboo table and making special pardons judgments in a single generation has a complexity of $O(N \cdot M)$. In the actual power SDN scenario, the number of neighborhood solutions M is much less than D, so the highest order term is still $O(G \cdot N \cdot D)$, and the overall complexity of TS-IGA is $O(G \cdot N \cdot D)$.

In conclusion, the research model optimizes the access performance through the fusion of multiple algorithms without increasing the algorithm's time complexity. It balances the optimization performance and computational efficiency, and has good practicality and implementation value in the real-time access scenario of power SDN.

5. Conclusion

To address the existing issues in power SDN systems, such as unreasonable hierarchical design, low real-time performance, and poor compatibility during controller access, this study developed two hybrid algorithms: PPO-FC-ACO and TS-IGA. These algorithms were used to achieve multi-level distributed control and optimize the access process of SDN controllers. By integrating both algorithms, an intelligent access model for power SDN controllers based on multi-level distributed control was constructed. The results showed that the model achieved a high load balancing degree of 0.898 and an access delay of only 33.4 ms. The decision consistency and load migration efficiency reached 97.4% and 97.8%. In field tests, the success rate of multi-level controller parallel access was 98.0%, with an average error as low as 1.51%. In addition, the interface matching rate remained above 80% when accessing a certain number and variety of controllers. Under conditions such as environmental interference, DoS attacks, and data tampering, the access decision response times were 143.6 ms, 182.0 ms, and 194.7 ms, respectively. However, the research still has the following limitations: Firstly, the proposed model has only been verified on the IEEE RTS-96 dataset and a small test platform, lacking exploration of scalability in large-scale heterogeneous power SDN, multi-operator cross-regional networking and other large-scale multi-regional systems, resulting in the need to verify the generalization performance of the model. Secondly, the security issues during the controller access process have not been considered, and there is a lack of security strategy design for the batch access of heterogeneous controllers and cross-regional data interaction. Thirdly, all experiments were conducted in an ideal link environment with stable bandwidth and no packet loss in communication, without considering the dynamic fluctuations of bandwidth and packet loss of communication data in real networks. In the future, a large-scale heterogeneous power SDN simulation and physical testing network covering multiple areas and nodes needs to be established. Typical scenarios such as regional expansion, cross-regional networking, and concurrent access of a large number of controllers should be simulated for testing to enhance the model's adaptability in complex wide-area power networks. Moreover, zero-trust architecture and blockchain technologies should be integrated to build an integrated security access mechanism to meet the high-security operation requirements of the power system. Additionally, real link conditions such as network bandwidth fluctuations and communication data packet losses should be simulated. Specialized tests and algorithm optimizations should be conducted for the differences in heterogeneous protocols of multiple controllers to further verify and improve the model's adaptability and robustness in complex engineering scenarios.

Acknowledgments
The research work in this paper was supported by the Science and Technology Project of China Southern Power Grid Company [Project No.: 030000KC23120100 (GDKJXM20231515)], for which we would like to express our gratitude.

References

[1] Shihab Hamad Khaleefah Al-Dulaim, Salama Mostafa, Saraswathy Shamini Gunasekaran, Umar Farooq Khattak, Siti Salwani Yaacob, Alde Alanda, et al. A deep learning-based fault detection and classification in smart electrical power transmission system. JOIV: International Journal on Informatics Visualization, March, 2024, **8**(2): 812-818.

[2] Alfan Presekal, Alexandru Stefanov, Vetrivel Rajkumar, Peter Palensky, et al. Attack graph model for cyber-physical power systems using hybrid deep learning. IEEE Transactions on Smart Grid, January, 2023, **14**(5): 4007-4020.

[3] Ricard Vilalta, Lluis Gifre, Ramon Casellas Raul Muñoz, Ricardo Martinez, Alberto Mozo, Antonio Pastor, Diego R. Lopez, Juan Pedro Fernández-Palacios, et al. Applying digital twins to optical networks with cloud-native SDN controllers. IEEE Communications Magazine, August, 2023, **61**(12): 128-134.

[4] Mohammed A. Awadallah, Sharif Naser Makhadmeh, Mohammed Azmi Al-Betar, Lamees Mohammad Dalbah, Aneesa Al-Redhaei, et al. Multi-objective ant colony optimization. Archives of Computational Methods in Engineering, September, 2025, **32**(2): 995-1037.

[5] Aslan and Erkin. An immune plasma algorithm based approach for UCAV path planning. Journal of King Saud University-Computer and Information Sciences, January, 2023, **35**(1): 56-69.

[6] Frdiesa. A controller placement algorithm using ant colony optimization in software-defined network. International Journal of Wireless Information Networks, March, 2024, **31**(2): 142-154.

[7] Yuesheng Tan, Jie Ouyang, Zhuo Zhang, Yinglun Lao, Pengju Wen, et al. Path planning for spot welding robots based on improved ant colony algorithm. Robotica, March, 2023, **41**(3): 926-938.

[8] Mani Sharifi, Ali Sayyad, Shareh Taghipour, Abdolreza Abhari, et al. Optimizing a joint reliability-redundancy allocation problem with common cause multi-state failures using immune algorithm. Proceedings of the Institution of Mechanical Engineers, Part O: Journal of Risk and Reliability, February, 2023, **237**(1): 152-165.

[9] Behera and Gangopadhyay. Evolving bijective S-Boxes using hybrid adaptive genetic algorithm with optimal cryptographic properties. Journal of Ambient Intelligence and Humanized Computing, March, 2023, **14**(3): 1713-1730.

[10] Anil Ram, Manash Pratim Dutta, Swarnendu Kumar Chakraborty, et al. A flow-based performance evaluation on RYU SDN controller. Journal of The Institution of Engineers (India): Series B, January, 2024, **105**(2): 203-215.

[11] Gagan Deep Singh, Vikas Tripathi, Ankur Dumka, Rajkumar Singh Rathore, Mohit Bajaj, José Escorcia-Gutierrez, Nojood O. Aljehane, Vojtěch Blažek, Lukas Prokop, et al. A novel framework for capacitated SDN controller placement: Balancing latency and reliability with PSO algorithm. Alexandria Engineering Journal, January, 2024, **87**: 77-92.

[12] Hafiz Usama Ishtiaq, Areeb Ahmed Bhutta, Adnan Noor Mian, et al. DHCP DoS and starvation attacks on SDN controllers and their mitigation. Journal of Computer Virology and Hacking Techniques, March, 2024, **20**(1): 15-25.

[13] Anil Kumar Bandani, Shaik Riyazuddien, Parameshachari B D, Sujata Patil, Arvind Ganesh, et al. Multiplicative long short-term memory-based software-defined networking for handover management in 5G network. Signal, Image and Video Processing, April, 2023, **17**(6): 2933-2941.

[14] Radu-Emil Precup, Anh-Tu Nguyen, Saso Blazic, et al. A survey on fuzzy control for mechatronics applications. International Journal of Systems Science, December, 2024, **55**(4): 771-813.

[15] Xu Zhongkai, Chu Chenyang, Xie Kai, Zhao Ruizhuo, Ke Wenjun, et al. Optimization Dispatch Method for High-proportion Renewable Energy Power Systems Based on SC-PPO. Journal of System Simulation, November, 2025, **37**(10): 2511-2521.

[16] Gyeong Ho Lee, Hyunseo Park, Jae Won Jang, Jaeseob Han, Jun kyun Choi, et al. PPO-based autonomous transmission period control system in IoT edge computing. IEEE Internet of Things Journal, July, 2023, **10**(24): 21705-21720.

[17] Yan Sun, Yin Wu, Yan Wu, Kai Liang, Cuihong Dong, Shiwei Liu, et al. Optimizing intelligent startup strategy of power system using PPO algorithm. Intelligent Decision Technologies, November, 2024, **18**(4): 3091-3104.

[18] Mansour and Al-hamdani. Tabu Search Algorithm to Optimize Layout Design for a Multi Objective Plant Function. Passer Journal of Basic and Applied Sciences, December, 2024, **6**(2): 446-452.

[19] Saida El Bakali, Hamid Ouadi, Giri Fouad, Saad Gheouany, Nada Mounir, Ismael Jrhilifa, et al. Tabu search algorithm for optimal electric water heating energy management. IFAC-PapersOnLine, July, 2024, **58**(13): 835-840.

[20] Junqi Zhang, Huan Liu, Peng Zu, Mengshi Zhao, Cheng

Wang, Aiiad Albeshri, Abdullah Abusorrah, MengChu Zhou, et al. Using tabu search to avoid concave obstacles for source location. IEEE Transactions on Intelligent Transportation Systems, July, 2023, **24**(11): 11720-11732.